Spin-exchange narrowing of the atomic ground-state resonances

W. Chalupczak,[1] P. Josephs-Franks,[1] B. Patton,[2] and S. Pustelny[2,3]
[1]*National Physical Laboratory, Hampton Road, Teddington TW11 0LW, United Kingdom*
[2]*Department of Physics, University of California at Berkeley, Berkeley, California 94720-7300, USA*
[3]*Institute of Physics, Jagiellonian University, Reymonta 4, 30-059 Kraków, Poland*
(Received 1 July 2014; revised manuscript received 14 August 2014; published 21 October 2014)

At the most fundamental level, the performance of atomic sensors is limited by quantum decoherence. The problem of decoherence has been addressed at low magnetic fields with atomic samples, where the limiting factor of the coherence lifetime arises from spin-exchange collisions. In this paper, we demonstrate the complex role of the collisions in the relaxation of quantum states of alkali-metal atoms. The detailed understanding of the collision role allows us to reduce the ground-state relaxation in stronger magnetic fields (tens μT). Reduction of the relaxation rate enables improvement of the performance of atomic sensors. In particular, enhancement of the sensitivity of optical magnetometers in the detection of stronger magnetic fields may be obtained. Reduced transverse relaxation also enables increasing quantum-information storage time in atomic vapor.

DOI: 10.1103/PhysRevA.90.042509 PACS number(s): 32.30.Bv, 32.60.+i, 32.70.Jz, 33.35.+r

Introduction. Some of the most sensitive measurements of physical quantities (e.g., time, frequency, magnetic field, etc.) utilize resonant interaction of light with atoms [1]. Recent progress in atomic sensors has been achieved through an improved understanding of the relaxation processes in such systems. In atomic vapors, the dominant relaxation, limiting the precision of measurements and the storage time of quantum information, is often determined by spin-exchange collisions (SECs). The SEC relaxation was extensively studied, both experimentally [2,3] and theoretically [4–6], in low magnetic fields. These studies resulted in the discovery of the so-called spin-exchange relaxation-free (SERF) regime, where the SEC relaxation is eliminated. Operation in the SERF regime enables observation of narrow optical resonances (hertz range) in high-density atomic vapors (10^{13}–10^{14} atoms/cm^3) [7,8], where the SEC rate exceeds the observed transverse relaxation rate by several orders of magnitude [9]. Recently, the same regime was demonstrated at low-density samples contained in alkene-coated vapor cells [10].

Narrowing of optical resonances in the SERF regime can be interpreted in generic terms of SEC-mediated coherence transfer between two ground-state hyperfine manifolds [11–13]. Efficiency of the transfer is subject to a resonance condition, which links the difference between relevant coherence frequencies and coherence relaxation rate [12]. If the size of the mismatch between coherence frequencies is comparable to the SEC relaxation rate, rapid SECs average out coherence precession with different Larmor frequencies, leading to a prolonged oscillation at the averaged frequency [4]. This manifests as the merging of respective spectral components in the detected signal [4] and reduction of their effective width. In alkali-metal atoms, where the Landé factors of two ground-state hyperfine states are nearly opposite, the nonzero magnetic field results in the departure from the resonance condition, leading to the advent of the SEC relaxation. This is the reason for the limitation of the SERF-magnetometer detection range to ultralow magnetic fields only [7].

In this paper, we identify a spin-exchange narrowing mechanism that works in magnetic fields up to tens of μT. It is based on SEC-driven coherence transfer between pairs of ground-state Zeeman sublevels within the same hyperfine manifold. Key to the observation is the implementation of indirect optical pumping [14]. In such a scheme, circularly polarized light (the pump) depletes a given hyperfine ground state, fully populating the other state, which is optically probed by a weak, linearly polarized light (probe). This hinders optical resonances from power broadening, but more importantly eliminates any relaxation arising from repopulation of the other hyperfine state (elimination of hyperfine relaxation). With our investigations, we find that the influence of SECs on the coherence relaxation varies considerably with the magnetic field, leading to the appearance of several regimes of SEC relaxation. Additionally, it is shown that at stronger magnetic field, where the resonance condition is not fulfilled due to the nonlinear Zeeman (NLZ) effect, the efficient coherence transfer may be reestablished by the employment of a tensor light shift. This results in the narrowing of the observed optical resonances and, in turn, may enhance the operation of atomic sensors, e.g., optical magnetometers. Our measurements are performed in a low-density atomic sample, i.e., the population distribution among the Zeeman sublevels is not governed by spin temperature. The experimental investigations are based on radio-frequency (rf) spectroscopy (see Ref. [16] and references therein), in which an rf scan yields the frequencies, relaxation, and amplitudes of the ground-state Zeeman coherences [17]. The setup, in which the measurements are performed, is shown in Fig. 1.

Relaxation magnetic field dependence. Figure 2 shows the magnetic field dependence (shown in terms of the Larmor frequency ν_L [18]) of the linewidths (full width at half maximum) of the two leading resonances of the rf spectrum (see inset to Fig. 2). The plots reveal several different magnetic-field regimes with distinct behavior of the widths. For the strongest magnetic fields ($\nu_L > 600$ kHz, regime I), the widths of the resonances do not change with the field, i.e., the transverse relaxation is magnetic-field independent [the dashed horizontal lines in Fig. 2(a) represent measured asymptotic values of the linewidths for the largest four resonances, $\Delta\nu^{\infty}_{i,i-1}$]. Below 600 kHz (regime II), the width increases until it reaches its maximum at around 300 kHz. The broadening is much more significant for the second largest resonance (see inset to Fig. 1), corresponding to the $\rho_{4-3,4-3}$

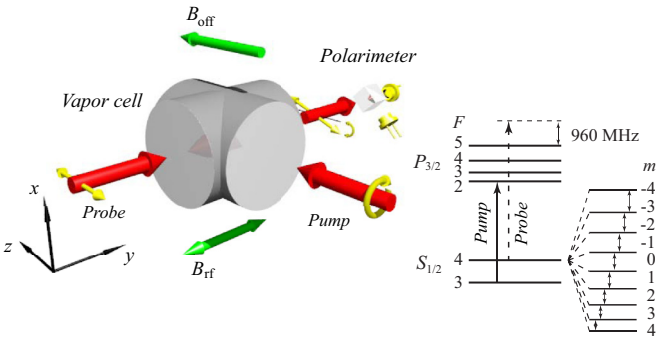

FIG. 1. (Color online) Geometry of the experiment. The Cs vapor is contained within an antirelaxation-coated glass cell. A 200 μW, circularly polarized laser light (pump) is tuned to the $F = 3 \rightarrow F' = 2$ component of the caesium D2 line (852 nm). The pump strongly polarizes the medium (polarization of the $F = 4$ ground state) along the offset magnetic field $B_{\rm off}$ via the so-called indirect optical pumping [14]. $B_{\rm off}$ splits magnetic sublevels that are coupled by the $\hat{y}$-polarized rf field of the amplitude $B_{\rm rf}$ (double-headed arrows in energy structure scheme). The state of the medium is detected by analyzing the polarization state of the off-resonant probe light that is detuned 1 GHz above the $F = 4 \rightarrow F' = 5$ transition (D2 line) propagating along $\hat{y}$. The whole system is enclosed inside a multilayer magnetic shield (not shown) with a shielding factor of 10^6. $B_{\rm off}$ is generated by a set of two solenoids situated inside the shield, providing the field with relative inhomogeneity of less than 10^{-5} over the length of the cell [15].

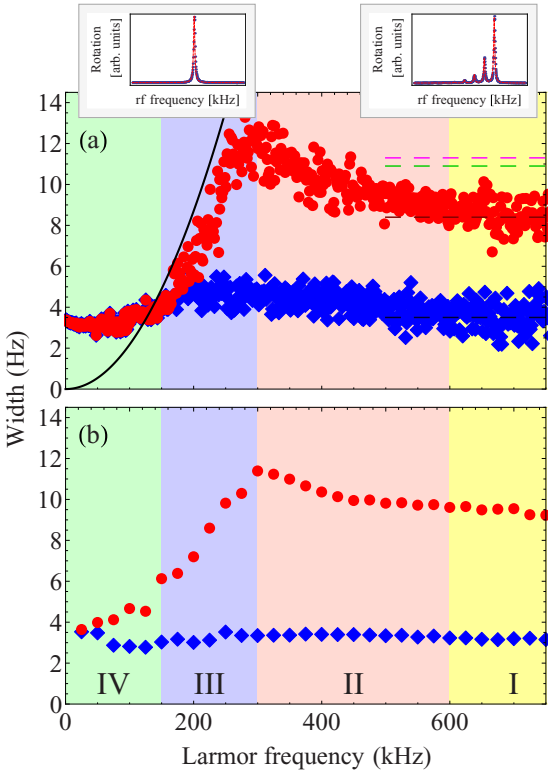

FIG. 2. (Color online) (a) Observed and (b) simulated widths of the resonances corresponding to the first two components of the rf spectrum as a function of the offset field (expressed in terms of the Larmor frequency). The signals were measured for a pump power of 200 μW, probe power of 15 μW, and atomic density of 1.1×10^{11} cm^{-3}, and the simulations were performed for corresponding physical conditions. The quadratic dependence (black solid line) shows separation of the lines (quadratic component of Zeeman effect), while the horizontal dashed lines represent measured asymptotic (high-field) values of the highest four peaks linewidths ($\Delta\nu^{\infty}_{-4,-3} = 3.5$ Hz, $\Delta\nu^{\infty}_{-3,-2} = 8.4$ Hz, $\Delta\nu^{\infty}_{-2,-1} = 10.9$ Hz, and $\Delta\nu^{\infty}_{-3,-2} = 11.3$ Hz). The numbers I–IV mark four regimes with different behavior of the relaxation rate on the magnetic field. The two insets show rf spectra measured at high and low magnetic fields, corresponding to split and unsplit rf spectra recorded in regimes I and II, and III and IV, respectively. The peak on the right represents $(-4, -3)$ coupling.

coherence (see discussion below), where it scales as ν_L^{-4}, than that to the $\rho_{4-4,4-3}$-coherence resonance. Below 300 kHz (regime III), the resonance widths narrow until the two resonances are characterized with the same linewidth (<160 kHz, regime IV).

To theoretically investigate the problem, density-matrix calculations are performed. The atomic structure of caesium is modeled by a four-level system with two ground states with $F = 3$ and $F = 4$ and two excited states with $F' = 2$ and $F' = 5$ (with appropriate Zeeman sublevel structure). Despite the larger number of excited states in a real atomic structure, the consideration of only two of the states corresponds well to the experimental condition, where these two excited levels are the most strongly excited due to the tuning of the pump and probe lasers. The modeling includes optical excitation with the pump light, coupling to the rf field, and interrogation by the probe beam. It also considers two types of relaxation: density-matrix independent (e.g., due to collisions with uncoated surfaces) and density-matrix dependent (e.g., due to SEC) relaxation. Based on the density-matrix approach, one can show that the signal (the angle of polarization rotation φ) is given by

$$\varphi \propto \sum_{j=-F}^{F-1} \langle F\, j+1\ 1\ 0|F'\, j+1\rangle \rho_{Fj,F'j+1} - \sum_{j=-F+1}^{F} \langle F\, j-1\ 1\ 0|F'\, j-1\rangle \rho_{Fj,F'j-1}, \qquad (1)$$

where $\rho_{Fj,F'j'}$ is the optical coherence between the $|Fj\rangle$ ground state and the $|F'j'\rangle$ excited state and $\langle|\rangle$ is the Clebsch-Gordan coefficient (the quantization axis is oriented along the offset magnetic field). Since the optical coherence $\rho_{Fj,F'j\pm1}$ depends on the ground-state Zeeman coherence $\rho_{Fj,Fj\pm1}$, the widths of the narrowest rf resonances are related to the lifetime of the ground-state coherences. In this respect, rf spectroscopy is an efficient tool in the investigations of the transverse relaxation, in particular SEC relaxation, being an important contribution to the relaxation.

Equation (1) and the dependence of the optical coherence on the Zeeman coherences show that in stronger magnetic fields, where nonlinear Zeeman effect unequally splits magnetic sublevels, rotation resonances are associated with specific Zeeman coherences. In particular, in the considered case, the strongest resonance (inset to Fig. 2) is related to the $\rho_{4-4,4-3}$ coherence and the second largest coherence arises due to the $\rho_{4-3,4-2}$ coherence.

The numerical simulations of the system fully replicate the experimentally measured behavior [Fig. 2(b)]. In particular, the linewidths of the simulated resonances first increase with the magnetic field, then decrease, eventually leveling up for higher magnetic fields. Similar to the experimental signal [Fig. 2(a)], the dependence of the linewidth of the resonance related to the $\rho_{4-3,4,-2}$ coherence is more pronounced than that arising from the $\rho_{4-4,4-3}$ coherence. This difference originates from the reduced SEC relaxation of the $|4-4\rangle$ state [19,20] and is the indication that the linewidths of the rf resonances are predominantly determined by SECs (except the $\Delta\nu_{-4-3}$ linewidth) [21]. As this paper investigates the role of SEC relaxation, below we exclusively concentrate on the relaxation of the $\rho_{4-3,4-2}$ coherence, extracted from the width of the second highest resonance.

For fields larger than 600 kHz (regime I), the overlap between components of the rf spectrum is negligible ($\Delta\nu_{\mathrm{NLZ}} \gg \max\{\Delta\nu_{-4,-3}, \Delta\nu_{-3,-2}, \ldots, \Delta\nu_{3,4}\}$). In such a case, the SEC contribution to the linewidth $\Delta\nu_{i,i+1}$ is exclusively given by the matrix element of the SEC operator ($H_{\mathrm{SE}} = J\mathbf{S}_1 \cdot \mathbf{S}_2$, where $\mathbf{S}_i$ is the electron spin operator of the atom, and J is the coupling coefficient) between two neighboring Zeeman sublevels $|F\ j\rangle$ and $|F\ j+1\rangle$ [5,6]. Since the SEC operator does not reveal any dependence on the magnetic field, increasing the field does not affect the linewidth of resonances $\Delta\nu^{\infty}_{i,i+1}$. This behavior can be intuitively understood as the collisional coherence transfer, leading to transverse relaxation; although coherence is preserved in SEC even at stronger fields, the coherence dephases after the collision due to the mismatch between the rf-field frequency, determining evolution of the rf-driven coherence (rf field in resonance with a given magnetic transition) and the uncoupled-coherence evolution frequency (the frequency mismatch between the rf-field frequency and the free evolution frequency significantly exceeds the transverse relaxation rate – the condition for the resonance coherence transferred is not fulfilled). At lower fields (regime II), the resonance frequencies are not well resolved, and the eigenvectors of the system's Hamiltonian become superpositions of the eigenvectors $|Fj\rangle$ [5]. Thereby, under such conditions, the relaxation rates of various coherences mix together and the width of a specific resonance is given by $\Delta\nu_{i,i+1}(\nu_L) = \Delta\nu^{\infty}_{i,i+1} + \sum_{j\neq i} f_j(\nu_L)\Delta\nu^{\infty}_{j,j+1}$, where $f_i(\nu_L)$ is the magnetic-field-dependent weight of a jth contribution. As the contributions from neighboring transitions increase with decreasing line separation, the ν_L^{-4} scaling of the resonance linewidth with the magnetic field, predicted theoretically [22], is observed. In the coherence-transfer language, this corresponds to the situation where most of the coherences are probed at once, and since they have different relaxation rates and their overlap depends on the magnetic field, the resonances have magnetic-field-dependent linewidths. It should be noted, however, that the leading resonance still does not contribute to the widths of other resonances as its width (3.5 Hz) is significantly smaller than the resonance separation in this magnetic field range ($\Delta\nu_{\mathrm{NLZ}}$ from 15 to 80 Hz). While at 300 kHz all but the leading resonance linewidths become equal, reaching their maximum value, the linewidths decrease quadratically while reducing the field (regime III). This occurs when the contribution of the $\rho_{4-4,4-3}$ coherence, being partially immune to SEC relaxation, becomes significant

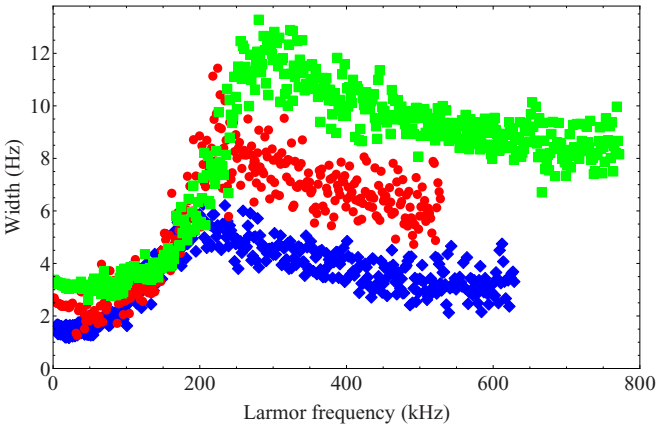

FIG. 3. (Color online) The field dependence of the resonance linewidth $\Delta\nu_{-3,-2}$ recorded at three different atomic densities: 0.4×10^{11} cm^{-3} (blue diamonds), 0.6×10^{11} cm^{-3} (red dots), 1.1×10^{11} cm^{-3} (green squares).

(overlapping between all resonances). Under such conditions, a coherence can be transferred to the $|4-4\rangle$ and $|4-3\rangle$ states, characterized with longer lifetime, where it is detectable. For even weaker fields ($\nu_L < 100$ kHz), there is no difference in resonance linewidths and no significant change of width $\Delta\nu_{i,i+1}$ due to the magnetic field that is observed (regime IV). For such a field range, all of the resonances overlap and the continuity of the coherent evolution is preserved after every SEC. As all the coherences are probed simultaneously, there is only one width of the observed signal mainly dominated by the relaxation of the $\rho_{4-4,4-3}$ coherence.

Since actual relaxation behavior depends upon the ratio of the separation between spectral profiles $\Delta\nu_{\mathrm{NLZ}}$ and the resonance linewidths $\Delta\nu_{i,i+1}$, it can be tuned by changing either the former, i.e., changing the offset magnetic field B_{off}, or the latter, e.g., by adjusting the cell temperature and hence atomic density. Figure 3 shows the linewidth $\Delta\nu_{-3,-2}$ as a function of the Larmor frequency recorded at three different vapor densities. At each density, the low-field linewidth is smaller than what would be predicted from the spin-exchange rate, which proves that mechanism of coherence transfer due to SECs at low fields is efficent. However, it should be noted that there is some residual SEC relaxation manifesting itself as changes of linewidths at zero magnetic field for various temperatures. This is due to incomplete elimination of the relaxation to the other hyperfine state in our indirect optical-pumping scheme (the light does not illuminate the cell completely). Additionally, the broadening may be caused by temperature-dependent deterioration of coating quality [23]. When the offset magnetic field increases, in all cases, the linewidth reveal the same behavior as discussed above, although maximum relaxation is obtained for different magnetic field, depending on vapor density.

Frequency dependence. In parallel with the dependence of the resonance linewidths, we also observed deviations in peak separation from the expected quadratic dependence on the field. Figure 4 shows the average separation of the components of the rf spectrum as a function of the amplitude of the offset field recorded at 1.1×10^{11} atoms/cm^3 and

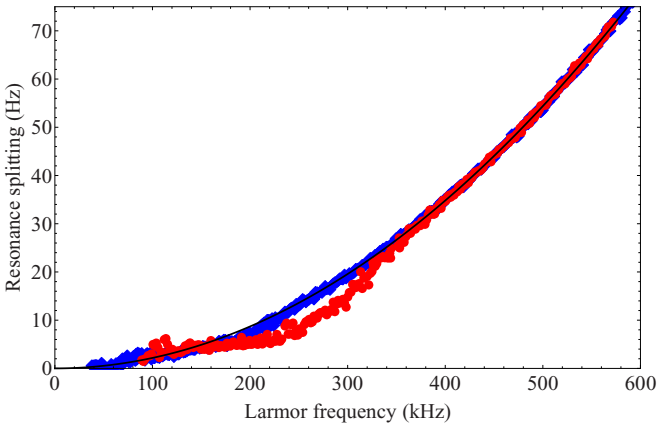

FIG. 4. (Color online) Average separation of the rf resonances as a function of the offset magnetic field (expressed in terms of the Larmor frequency) recorded at atomic densities 1.1×10^{11} atoms/cm^3 (red squares) and 2.1×10^{11} atoms/cm^3 (blue dots). The results reveal deviations from the magnetic-sublevel splittings predicted by the Breit-Rabi equation (solid black line).

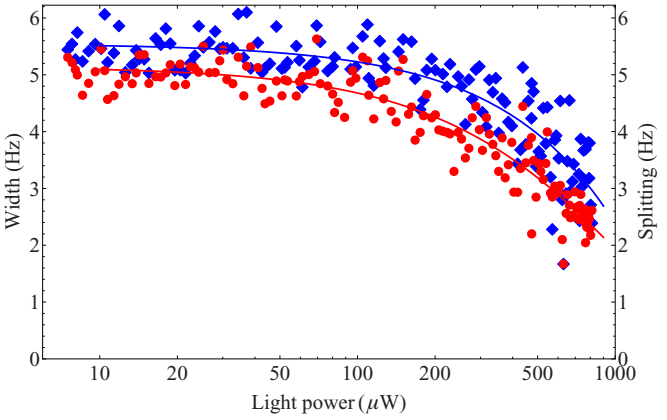

FIG. 5. (Color online) Width (blue diamonds) of rf spectral profile, $\Delta\nu_{-3,-2}$, recorded at 165 kHz as a function of power of the laser beam that generates tensor light shift (atomic densities 0.3×10^{11} atoms/cm^3). Red squares show averaged peak separation (nonlinear splitting of the sublevels). Solid lines are the trend lines to guide the eye.

2.1×10^{11} atoms/cm^3. In particular, for the same data set as presented in Fig. 2 (red squares), for $\nu_L < 300$ kHz, where quadratic dependence of $\Delta\nu_{-3,-2}$ on ν_L has been observed, the separation is smaller than the value of quadratic splitting of the resonances (solid black line). This change in the line separation is yet another signature of the coherence-transfer mechanism (see Ref. [4] for more details).

Narrowing resonances. Since the increased linewidth at higher magnetic fields results from the dephasing of the coherence due to the nonlinear Zeeman splitting exceeding the spin-exchange rate, one would expect that compensation of $\Delta\nu_{\mathrm{NLZ}}$ via, for example, a tensor light shift would result in resonance narrowing. We have performed experiments demonstrating the influence of the compensation of $\Delta\nu_{\mathrm{NLZ}}$ with tensor light shift on linewidths in a configuration similar to that described in Ref. [24]. Apart from the pump and probe lasers, a third laser, detuned 2 GHz from the $F = 4 \rightarrow F' = 3$ transition of the caesium D1 line (894 nm), was also used. The observation was done with atomic density of 0.4×10^{11} cm^{-3} (blue dots in Fig. 3) and a magnetic field set to a value equivalent to a Larmor frequency of 165 kHz. The particular choice of operating conditions enabled us to demonstrate all of the processes relevant to the cancellation of $\Delta\nu_{\mathrm{NLZ}}$ by a tensor light shift. Figure 5 presents the dependence of $\Delta\nu_{-3,-2}$ (green diamonds) on the power of the laser which generates the tensor light shift. In addition to the width dependence, the plot additionally shows the average peak separation which is a measure of the compensation. As pointed out in Ref. [24], implementation of the intense laser beam, generating a tensor light shift that does not cover the total aperture of the atomic cell, could lead to broadening of the resonances. In our experiment, the laser beam which creates the tensor light shift only partially covered the aperture of the cell window. Thus, the narrowing effect was masked (totally in the case of $\Delta\nu_{-4,-3}$ and partially in case of $\Delta\nu_{-3,-2}$) by the broadening caused by the inhomogeneity of the laser field across the cell.

Conclusions. Changes of SEC relaxation across a wide range of magnetic fields have been discussed. Since the lifetime of the ground-state coherences limited by SEC relaxation defines, at a fundamental level, the precision of magnetic field measurements performed with such systems, an understanding of the mechanisms of this relaxation-rate change with magnetic field paves the way to a broader implementation of ultrasensitive magnetic field sensors [25]. Immediate applications of the discussed effect could be in atomic magnetometers operating in the radio-frequency domain (e.g., nuclear magnetic resonance [26], nuclear quadrupole resonance [27], etc.). However, the importance of long-lived ground-state coherences in alkali-metal atoms extends beyond the field of nuclear resonance. The narrow ground-state coherence lines have been exploited in several areas of modern physics, including fundamental physics (Lorentz invariance [28]), metrology (clocks based on end resonances [29]), quantum-information processing (continuous variable systems [30]), and cosmology (search for domain walls formed by axionlike fields [31]).

Acknowledgments. The work was funded by UK Department for Business, Innovation and Skills as part of the National Measurement System Programme and U.K. MOD Science and Technology Programme (Contract No. DSTL/AGR/00315/01). S.P. acknowledges the support of the Polish National Centre for Research and Development within the Leader Program (Grant No. LIDER/025/571/L-4/12/NCBR/2013).

[1] D. Budker and M. V. Romalis, Nat. Phys. **3**, 227 (2007).
[2] W. Happer and H. Tang, Phys. Rev. Lett. **31**, 273 (1973).
[3] I. M. Savukov and M. V. Romalis, Phys. Rev. A **71**, 023405 (2005).

[4] W. Happer and A. C. Tam, Phys. Rev. A **16**, 1877 (1977).

[5] S. Appelt, A. Ben-Amar Baranga, C. J. Erickson, M. V. Romalis, A. R. Young, and W. Happer, Phys. Rev. A **58**, 1412 (1998); S. J. Smullin, I. M. Savukov, G. Vasilakis, R. K. Ghosh, and M. V. Romalis, *ibid.* **80**, 033420 (2009).

[6] D. K. Walter and W. Happer, Laser Phys. **12**, 1182 (2002).

[7] I. K. Kominis, T. W. Kornack, J. C. Allred, and M. V. Romalis, Nature (London) **422**, 596 (2003).

[8] M. P. Ledbetter, I. M. Savukov, V. M. Acosta, D. Budker, and M. V. Romalis, Phys. Rev. A **77**, 033408 (2008).

[9] Reduction of SEC broadening at higher magnetic fields could be achieved by optical pumping of atoms to the maximum angular momentum state [5]. This paper's focus is on the alternative mechanism of SEC relaxation to optical pumping.

[10] M. V. Balabas, T. Karaulanov, M. P. Ledbetter, and D. Budker, Phys. Rev. Lett. **105**, 070801 (2010).

[11] G. A. Ruff and T. R. Carver, Phys. Rev. Lett. **15**, 282 (1965).

[12] S. Haroche and C. Cohen-Tannoudji, Phys. Rev. Lett. **24**, 974 (1970).

[13] J. Skalla, G. Wackerle, and M. Mehring, Opt. Commun. **127**, 31 (1996).

[14] W. Chalupczak, R. M. Godun, P. Anielski, A. Wojciechowski, S. Pustelny, and W. Gawlik, Phys. Rev. A **85**, 043402 (2012).

[15] The line broadening caused by magnetic field gradients has been determined and subtracted from the data presented here.

[16] D. Budker and D. F. Jackson Kimball, *Optical Magnetometry* (Cambridge University Press, Cambridge, 2013).

[17] At higher offset magnetic fields, when the signal splits into several resonances, the fitting that enables determination of the amplitudes and widths of all individual resonances is straightforward. The resonance amplitude ratios are constant in Larmor frequency range 200–770 kHz (for measurement conditions as in Fig. 2). The assumption is made that they remain unchanged below 200 kHz, where resonances are unsplit, so that only one amplitude is a free parameter in our fitting.

[18] The Larmor frequency ν_L is related to the magnetic field $B_{\rm off}$ via $\nu_L = g\mu_B B_{\rm off}/h$, where g is the Landé factor, μ_B is the Bohr magneton, and h denotes the Planck constant.

[19] For strongly polarized systems, where most of the atomic population resides in the $|4-4\rangle$ state, SEC relaxation is strongly suppressed. This effect leads to narrowing of optical resonances and is known as optical narrowing [5,14].

[20] S. Appelt, A. Ben-Amar Baranga, A. R. Young, and W. Happer, Phys. Rev. A **59**, 2078 (1999).

[21] We have confirmed, with independent measurements, relaxation in the dark, as in M. T. Graf, D. F. Kimball, S. M. Rochester, K. Kerner, C. Wong, D. Budker, E. B. Alexandrov, M. V. Balabas, and V. V. Yashchuk, Phys. Rev. A **72**, 023401 (2005); that while the rf resonance widths experience quite distinct change with the magnetic field, the longitudinal relaxation is unaffected with the magnetic field.

[22] A. V. Taichenachev, V. I. Yudin, C. W. Oates, C. W. Hoyt, Z. W. Barber, and L. Hollberg, Phys. Rev. Lett. **96**, 083001 (2006).

[23] S. Pustelny, A. Wojciechowski, M. Gring, M. Kotyrba, J. Zachorowski, and W. Gawlik, J. Appl. Phys. **103**, 063108 (2008).

[24] K. Jensen, V. M. Acosta, J. M. Higbie, M. P. Ledbetter, S. M. Rochester, and D. Budker, Phys. Rev. A **79**, 023406 (2009).

[25] Low density of the atomic sample (1.2×10^{11} atoms/cm^{-3}) does not prevent a sensor from reaching high sensitivity (e.g., rf atomic magnetometer described in W. Chalupczak, R. M. Godun, S. Pustelny, and W. Gawlik, Appl. Phys. Lett. **100**, 242401 (2012), with demonstrated sensitivity at 1.16 f T/Hz$^{1/2}$ level). As shown in V. Shah, G. Vasilakis, and M. V. Romalis, Phys. Rev. Lett. **104**, 013601 (2010), the problem of bandwidth in magnetometers with narrow spectral profiles can be addressed in a quantum non-demolition measurement configuration.

[26] M. P. Ledbetter, T.. Theis, J. W. Blanchard, H. Ring, P. Ganssle, S. Appelt, B. Blumich, A. Pines, and D. Budker, Phys. Rev. Lett. **107**, 107601 (2011).

[27] S.-K. Lee, K. L. Sauer, S. J. Seltzer, O. Alem, and M. V. Romalis, Appl. Phys. Lett. **89**, 214106 (2006).

[28] M. Smiciklas, J. M. Brown, L. W. Cheuk, S. J. Smullin, and M. V. Romalis, Phys. Rev. Lett. **107**, 171604 (2011).

[29] Y.-Y. Jau, A. B. Post, N. N. Kuzma, A. M. Braun, M. V. Romalis, and W. Happer, Phys. Rev. Lett. **92**, 110801 (2004).

[30] J. F. Sherson, H. Krauter, R. K. Olsson, B. Julsgaard, K. Hammerer, I. Cirac, and E. S. Polzik, Nature (London) **443**, 557 (2006).

[31] M. Pospelov, S. Pustelny, M. P. Ledbetter, D. F. Jackson Kimball, W. Gawlik, and D. Budker, Phys. Rev. Lett. **110**, 021803 (2013).